

# Fractional Langevin Equation Driven by Multifractional Brownian Motion: Integral Equation Approach

Jincheng Dong<sup>2</sup>, Ning Du<sup>2</sup> and Zhiwei Yang<sup>1,\*</sup>

<sup>1</sup>*School of Qilu Transportation and State Key Laboratory of  
Intelligent Manufacturing of Advanced Construction Machinery,  
Shandong University, Jinan 250002, China.*

<sup>2</sup>*School of Mathematics, Shandong University, Jinan 250100, China.*

*Received 30 October 2025; Accepted (in revised version) 31 January 2026.*

---

**Abstract.** The fractional Langevin stochastic differential equation driven by multifractional Brownian motion of Riemann-Liouville type, which describes the long-range interactions and its mean square displacement has a power-law growth in time  $\langle x^2(t) \rangle \simeq t^\alpha$ , where  $0 < \alpha < 1$  correspond to the subdiffusion, and  $\alpha$  is the fractional order. In this paper, we extend the framework to account for time-varying environmental properties, leading to a variable-order fractional Langevin equation. We give the Euler-Maruyama scheme of the solution and then prove the strong convergence of the Euler-Maruyama scheme. Numerical experiments with time-dependent Hurst indices are presented to illustrate the theoretical findings.

**AMS subject classifications:** 60H10, 65C30

**Key words:** Fractional Langevin equation, multifractional Brownian motion, power-law, existence and uniqueness, Euler-Maruyama method.

---

## 1. Introduction

The classical Langevin equation (CLE) is usually applied to describe the random motion of the Brownian particle during the ideal environment according to the Newton's laws [4, 5, 9, 10, 15, 21]. The driving force for the motion of the particle comes from a rapidly fluctuating force  $\mathcal{F}(t)$ , which called the white noise with the expectation and correlation function

$$\langle \mathcal{F}(t) \rangle = 0, \quad \langle \mathcal{F}(t_1), \mathcal{F}(t_2) \rangle \simeq \delta(t_1 - t_2).$$

We consider the particle of mass  $m$  and  $x(t)$  denotes the displacement. A viscous drag  $-\sigma(dx/dt)$  represents a dynamical frictional experienced by the particle, and  $\sigma$  is the

---

\*Corresponding author. *Email address:* zhiweiyang@sdu.edu.cn (Z. Yang)

coefficient of friction. Thus, one may apply the second Newton's law to derive the motion of a particle by the following CLE:

$$m \frac{d^2 x(t)}{dt^2} + \sigma \frac{dx(t)}{dt} = \mathcal{F}(t) \quad (1.1)$$

with  $x(0) = x_0$  and  $x'(0) = \hat{x}_0$ . This model can simulate standard diffusion process such that the mean square displacement (MSD) satisfies the relation

$$\langle x^2(t) \rangle \simeq t.$$

Using the notation

$$\mathcal{F}(t) = \frac{d\mathcal{B}(t)}{dt}, \quad v(t) = \frac{dx(t)}{dt},$$

we can rewrite (1.1) as

$$mdv + \sigma v(t)dt = d\mathcal{B}(t), \quad (1.2)$$

where  $\mathcal{B}(t)$  is a standard Brownian motion.

However, when the particle immersed in the non-ideal environment, such as in the viscoelastic liquids, and the damping friction is no longer a linear friction relationship. Hence, the motion of the particle is characterized as anomalous diffusion processes [8, 12, 13, 19]. Under this circumstance, the classical equations (1.1) cannot describe such anomalous diffusion processes well. As a matter of fact, the motion of the particle can be described by the generalized Langevin equation

$$m \frac{d^2 x(t)}{dt^2} + \sigma \int_0^t c(t-s)x'(s)ds = \mathcal{G}(t),$$

where  $c(t)$  represents the memory effect and  $\mathcal{G}(t)$  is no longer a white noise. We focus on the fractional Gaussian noise with

$$\langle \mathcal{G}(t) \rangle = 0, \quad \langle \mathcal{G}(0), \mathcal{G}(t) \rangle \simeq t^{-\alpha}, \quad \alpha \in (0, 1).$$

Fractional Brownian motion (FBM) based on the Riemann-Liouville fractional type is defined by [1, 20]

$$\mathcal{B}_H(t) = \int_0^t \frac{(t-s)^{H-1/2}}{\Gamma(H+1/2)} d\mathcal{B}(s), \quad t \geq 0,$$

where  $H$  represent the Hurst index of the fractal. We use the Caputo fractional derivative operator  $D_t^\alpha$  by setting  $\alpha = 2 - 2H$ ,  $1/2 < H < 1$  to arrive at the fractional Langevin stochastic differential equation (FLE)

$$m \frac{d^2 x(t)}{dt^2} + \sigma D_t^\alpha x(t) = \mathcal{G}(t), \quad \alpha \in (0, 1), \quad (1.3)$$

where the fractional derivative is defined by [22]

$$D_t^\alpha g(t) := \int_0^t \frac{(t-s)^{-\alpha}}{\Gamma(1-\alpha)} g'(s)ds.$$

Fractional differential equations have gained significant attention and found important applications across various fields in recent years [6, 11, 14, 16, 23, 26, 29]. This model can simulate the subdiffusion process, which means the MSD has the following form — cf. [19]:

$$\langle x^2(t) \rangle \simeq t^\alpha.$$

Finally we can substitute  $\mathcal{G}(t)$  by  $d\mathcal{B}_H(t)/dt$  to reformulate (1.3) as follows:

$$mdv(t) + \sigma \int_0^t c(t,s)v(s)dsdt = d\mathcal{B}_H(t), \quad (1.4)$$

where  $\mathcal{B}_H(t)$  represents the FBM and

$$c(t,s) = \frac{1}{\Gamma(1-\alpha)}(t-s)^{-\alpha}.$$

We note that if  $\alpha \rightarrow 1$  ( $H \rightarrow 0.5$ ) then the FLE (1.3) and (1.4) return to the classical CLE (1.1), (1.2) respectively

$$\text{FLE} \xrightarrow{\alpha \rightarrow 1 (H \rightarrow 0.5)} \text{CLE}.$$

Fig. 1 shows that when  $\alpha = 0.3, 0.6, 0.9$  respectively (at this time  $H = 0.85, 0.7, 0.55$ ), the MSD of the Eq. (1.4) presents different power-law grows in time. Fig. 2 shows that when  $\alpha \rightarrow 1$ ,  $H \rightarrow 0.5$ , the relationship between the MSD and time of the Eq. (1.4) approaches a linear relationship (the slope approaches 1), and (1.4) approaches an integer-order stochastic differential equation driven by white noise.

In more general scenarios, the surrounding medium of the particle may change during the diffusion [24, 27, 28, 30, 31], which will lead to the change of the Hurst index. Hence, we derive at a variable-order fractional Langevin equation. Based on the above considerations, we consider a generalization of (1.3) by incorporating the transient velocity-dependent external forces  $f(v(t))$ , such forces motivated by the modeling of non-conservative effects such as friction, damping, or feedback control, which naturally depend on the instantaneous

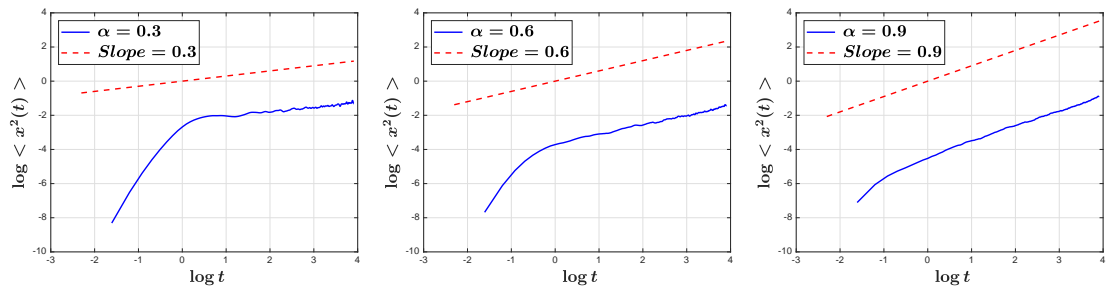


Figure 1: The plots of the MSD  $\langle x^2(t) \rangle$  for the fractional Langevin equation driven by FBM with  $\alpha = 0.3, 0.6, 0.9$  ( $H = 0.85, 0.7, 0.55$ ), respectively. And the discrete parameters are  $T = 50, \Delta t = 0.1, M = 1000$ .

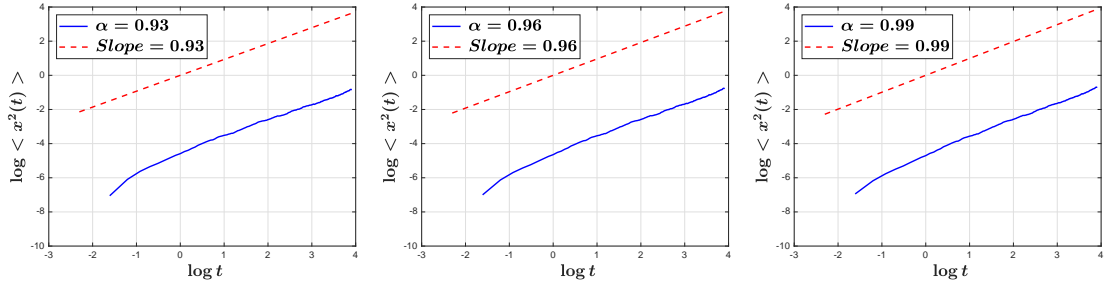


Figure 2: The plots of the MSD  $\langle x^2(t) \rangle$  for the fractional Langevin equation driven by FBM with  $\alpha = 0.93, 0.96, 0.99 \rightarrow 1$  ( $H = 0.535, 0.520, 0.505 \rightarrow 0.5$ ), respectively. And the discrete parameters are  $T = 50, \Delta t = 0.1, M = 1000$ .

velocity rather than the displacement. Our variable-order fractional Langevin equation (VFLE) with  $m = 1$  can be expressed as

$$\frac{d^2x(t)}{dt^2} + \sigma D_t^{\alpha(t)}x(t) = f(v(t)) + \frac{d\mathcal{W}_H(t)}{dt},$$

$$\alpha(t) = 2 - 2H(t) \in (0, 1) \quad \text{and} \quad H(t) \in \left(\frac{1}{2}, 1\right),$$

where  $f$  represents the external force. The multifractional Brownian motion  $\mathcal{W}_H(t)$  is defined by [20]

$$\mathcal{W}_H(t) = \int_0^t \frac{1}{\Gamma(H(t) + 1/2)} (t-s)^{H(t)-1/2} d\mathcal{B}(s), \quad t \geq 0, \quad (1.5)$$

and the variable fractional derivative is given by [22]

$$D_t^{\alpha(t)}g(t) := \int_0^t \frac{(t-s)^{-\alpha(s)}}{\Gamma(1-\alpha(s))} g'(s) ds.$$

Applying  $dx(t) = v(t)dt$  and considering the variable external force  $f(v(s))$ , then we arrive at the variable-order fractional Langevin equation

$$dv(t) = -\sigma \int_0^t \frac{(t-s)^{-\alpha(s)}}{\Gamma(1-\alpha(s))} v(s) ds dt + f)dt + d\mathcal{W}_H(t), \quad (1.6)$$

with  $v(0) = x'(0) = \hat{x}_0$  and  $x(0) = x_0$ .

It is difficult to obtain analytical solutions of the VFLE (1.6), so we develop numerical scheme for approaching the solutions. We present an Euler-Maruyama (EM) scheme of (1.6) and propose its strong convergence. In Section 2, we first recall several auxiliary lemmas from the existing literature, which will be repeatedly used in our subsequent analysis. Based on these results, we then prove the existence and uniqueness of solutions to the VFLE (1.6). In Section 3, an EM approximation is developed for the proposed model and the corresponding strong convergence is proved. In Section 4, numerical experiments are performed to support the theoretically predicted convergence rate.

## 2. Existence and Uniqueness of Solutions to VFLE

### 2.1. Preliminaries

To establish our main results and lay the foundation for the subsequent numerical analysis, we begin by presenting several essential lemmas and assumptions that will be used throughout this paper.

**Lemma 2.1** (Jensen Inequality, cf. Lord *et al.* [17]). *For any concave function  $\phi : [0, \infty) \rightarrow \mathbb{R}$  with  $\phi(0) \geq 0$ , the following inequality holds:*

$$\phi\left(\sum_{i=1}^n x_i\right) \leq \sum_{i=1}^n \phi(x_i).$$

**Lemma 2.2** (Cauchy Inequality, cf. Oksendal [17]). *Let  $f, g \in L^2([a, b])$ . Then*

$$\int_a^b |f(t)g(t)| dt \leq \left(\int_a^b |f(t)|^2 dt\right)^{1/2} \left(\int_a^b |g(t)|^2 dt\right)^{1/2}.$$

**Lemma 2.3** (Chebyshev Inequality, cf. Oksendal [17]). *Let  $X$  be a random variable such that  $\mathbb{E}[|X|^p] < \infty$  for some  $p > 0$ . Then for any  $a > 0$ ,*

$$\mathbb{P}(|X| \geq a) \leq \frac{\mathbb{E}[|X|^p]}{a^p}.$$

**Lemma 2.4** (Burkholder-Davis-Gundy Inequality, cf. Le Gall [10]). *Suppose  $M(t)$  is a continuous local martingale on the interval  $[0, T]$ , then there exist a constant  $\bar{Q}_1$  depending on  $p$  such that, for  $1 \leq p < \infty$ ,*

$$\mathbb{E}\left[\left(\sup_{t \in [0, T]} |M(t)|\right)^p\right] \leq \bar{Q}_1 \mathbb{E}\left[\left([M, M](T)\right)^{p/2}\right],$$

where  $[G, G](t)$  is the quadratic variation process of  $\mathcal{G}(t)$ .

**Lemma 2.5** (Borel-Cantelli Lemma, cf. Mao [18]). *Let  $\{A_n\}_{n=1}^{\infty}$  be events in a probability such that  $\sum_{n=1}^{\infty} \mathbb{P}(A_n) < \infty$ , then*

$$\mathbb{P}(A_n \text{ i.o.}) < \infty,$$

where  $A_n$  i.o. is defined by  $\bigcap_{n=1}^{\infty} \bigcup_{m=n}^{\infty} A_m$ .

**Lemma 2.6** (Gronwall Inequality, cf. Brunner [3]). *Let  $\bar{Q}_0(t)$  be a non-negative and non-decreasing locally integrable function on  $[a, b]$ ,  $\bar{Q}_1 \geq 0$  be a constant. Suppose  $q(t)$  is a non-negative locally integrable function on  $[a, b)$  with*

$$q(t) \leq \bar{Q}_0(t) + \bar{Q}_1 \int_a^t q(s) ds, \quad \forall t \in [a, b),$$

then

$$q(t) \leq \bar{Q}_0(t) \exp(\bar{Q}_1(t-a)), \quad \forall t \in [a, b).$$

**Lemma 2.7** (Differentiation Rule, cf. Berger *et al.* [2, Corollary 4.B]). *Let  $\mathcal{B}(t)$  be a Brownian motion and  $f(t, s)$  be defined and measurable on  $\mathfrak{F} \times \Omega$  with values in  $\mathbb{R}^d \otimes \mathbb{R}^m$ , where*

$$\mathfrak{F} = \{(t, s) \in [t_0, T] \times [t_0, T] : s < t\}.$$

*Assume that  $f(t, s)$  is nonanticipating in  $s$  for each  $t \in [t_0, T]$ , and that for each  $t \in [t_0, T]$ ,*

$$\int_{t_0}^t |f(t, s)|^2 ds < \infty, \quad \text{a.s.}$$

*Suppose further that  $f$  is almost surely absolutely continuous in  $t$ , and satisfies*

$$\int \int_{\mathfrak{F}} \left| \frac{\partial}{\partial t} f(t, s) \right|^2 ds dt < \infty, \quad \text{a.s.}$$

*Define the stochastic process*

$$x(t) = \int_{t_0}^t f(t, s) d\mathcal{B}(s), \quad t \in [t_0, T].$$

*Then*

$$dx(t) = f(t, t) d\mathcal{B}(t) + \left[ \int_{t_0}^t \frac{\partial}{\partial t} f(t, s) d\mathcal{B}(s) \right] dt.$$

**Lemma 2.8** (Stochastic Fubini Theorem, cf. Berger *et al.* [2, Theorem 4.A]). *Let  $\mathcal{B}(t)$  be a Brownian motion and  $\mathcal{J}$  be any bounded Borel set in the first quadrant of the  $(t, s)$  plane. Let  $f$  be defined and measurable on  $\mathcal{J} \times \Omega$  with values in  $\mathbb{R}^d \otimes \mathbb{R}^m$ . Let  $f(t, s)$  be nonanticipating in  $s$  for each  $t$ . If*

$$\int_{\mathcal{J}} |f(t, s)|^2 ds dt < \infty, \quad \text{a.s.},$$

*then*

$$\int \int_{\mathcal{J}} f(t, s) d\mathcal{B}(s) dt = \int \int_{\mathcal{J}} f(t, s) dt d\mathcal{B}(s).$$

The data of (1.6) are assumed to satisfy the following conditions.

**Assumption 2.1.**  $H(t) \in C^1[0, T]$  on  $[0, T]$  with  $1/2 < H_{\min} \leq H(t) \leq H_{\max} < 1$ .

**Assumption 2.2** (Lipschitz Condition). There exists  $L > 0$ , such that for all  $v, \tilde{v} \in \mathbb{R}$ ,

$$|f(v) - f(\tilde{v})|^2 \leq L|v - \tilde{v}|^2.$$

**Assumption 2.3** (Growth Condition). There exists  $L > 0$  such that for all  $v \in \mathbb{R}$ ,

$$|f(v)|^2 \leq L(1 + |v|^2).$$

## 2.2. Reformulation of the VFLE

Let

$$c_1(t, s) := \frac{(t-s)^{2H(s)-1}}{\Gamma(2H(s))}, \quad c_2(t, s) := \frac{(t-s)^{H(t)-0.5}}{\Gamma(H(t)+0.5)}.$$

We apply the relation  $\alpha(s) = 2 - 2H(s)$  to have

$$\int_0^t \int_0^s \frac{(s-r)^{-\alpha(r)}}{\Gamma(1-\alpha(r))} v(r) dr ds = \int_0^t \frac{(t-r)^{1-\alpha(r)}}{\Gamma(2-\alpha(r))} v(r) dr = \int_0^t c_1(t, s) v(s) ds.$$

Since  $H(t) > H_{\min} > 1/2$ , then  $c_2(t, t) = 0$ . Using the differentiation rule for stochastic processes (1.5), we obtain

$$d\mathcal{W}_H(t) = \left[ \int_0^t \frac{\partial c_2}{\partial t}(t, s) d\mathcal{B}(s) \right] dt.$$

Using the stochastic Fubini theorem to obtain

$$\int_0^t d\mathcal{W}_H(s) = \int_0^t \left[ \int_0^u \frac{\partial c_2}{\partial u}(u, v) d\mathcal{B}(v) \right] du = \int_0^t \left[ \int_v^t \frac{\partial c_2}{\partial u}(u, v) du \right] d\mathcal{B}(v),$$

and hence

$$\int_0^t d\mathcal{W}_H(s) = \int_0^t c_2(t, v) d\mathcal{B}(v) = \mathcal{W}_H(t).$$

Integral the model problem (1.6) from 0 to  $t$  to arrive at

$$v(t) = v(0) - \sigma \int_0^t c_1(t, s) v(s) ds + \int_0^t f(v(s)) ds + \int_0^t c_2(t, s) d\mathcal{B}(s). \quad (2.1)$$

Since  $\Gamma(z)$  is increasing on  $(1, 2)$  and  $\Gamma(2H(s)) > 0.5$ , we can estimate  $c_1(t, s)$  as

$$|c_1(t, s)| = \frac{(t-s)^{2H(s)-1}}{\Gamma(2H(s))} < 2(t-s)^{2H(s)-1} \leq Q_0, \quad Q_0 = \max\{2, 2T\}. \quad (2.2)$$

Similarly,

$$|c_2(t, s)| = \frac{(t-s)^{H(t)-0.5}}{\Gamma(H(t)+0.5)} < 2(t-s)^{H(t)-0.5} < Q_1, \quad Q_1 = \max\{2, 2\sqrt{T}\}. \quad (2.3)$$

**Theorem 2.1.** *Under Assumptions 2.1-2.3, the Eq. (2.1) has a unique solution  $v$  such that*

$$\mathbb{E} \left[ \sup_{0 \leq s \leq t} |v(s)|^2 \right] \leq Q_2 \exp(Q_3 t) < \infty, \quad t \in [0, T],$$

where

$$Q_2 = 4\mathbb{E}[v_0^2] + 4LT(T + Q_1^2), \quad Q_3 = 4(TQ_0^2\sigma^2 + LT). \quad (2.4)$$

*Proof.* Define a sequence  $\{p_n\}_{n=0}^{\infty}$  by  $p_0(t) = v_0$  and for  $n \geq 1$ ,

$$p_n(t) = v_0 - \sigma \int_0^t c_1(t, s) p_{n-1}(s) ds + \int_0^t f(p_{n-1}(s)) ds + \int_0^t c_2(t, s) d\mathcal{B}(s).$$

If  $n \geq 0$  and  $t \in [0, T]$ , then

$$p_{n+1}(t) - p_n(t) = -\sigma \int_0^t (p_n(s) - p_{n-1}(s)) c_1(t, s) ds + \int_0^t f(p_n(s)) - f(p_{n-1}(s)) ds.$$

Taking into account Jensen inequality, we write

$$\begin{aligned} & \mathbb{E} \left[ \sup_{0 \leq s \leq t} |p_{n+1}(s) - p_n(s)|^2 \right] \\ & \leq 2\mathbb{E} \left[ \sup_{0 \leq s \leq t} \left| \sigma \int_0^s c_1(s, r) (p_n(r) - p_{n-1}(r)) dr \right|^2 \right] \\ & \quad + 2\mathbb{E} \left[ \sup_{0 \leq s \leq t} \left| \int_0^s f(p_n(r)) - f(p_{n-1}(r)) dr \right|^2 \right] \\ & =: G_1 + G_2. \end{aligned} \tag{2.5}$$

The Cauchy inequality and the estimate (2.2) give

$$\begin{aligned} G_1 & \leq 2\mathbb{E} \left[ \sigma^2 \sup_{0 \leq s \leq t} \int_0^s |c_1(s, r)|^2 dr \int_0^s |p_n(r) - p_{n-1}(r)|^2 dr \right] \\ & \leq 2t\sigma^2 Q_0^2 \int_0^t \mathbb{E} \left[ \sup_{0 \leq r \leq s} |p_n(r) - p_{n-1}(r)|^2 \right] ds. \end{aligned} \tag{2.6}$$

By the Cauchy inequality and Assumption 2.2, we have

$$\begin{aligned} G_2 & \leq 2t\mathbb{E} \left[ \sup_{0 \leq s \leq t} \int_0^s |f(p_n(s)) - f(p_{n-1}(s))|^2 ds \right] \\ & \leq 2tL \int_0^t \mathbb{E} \left[ \sup_{0 \leq r \leq s} |p_n(r) - p_{n-1}(r)|^2 \right] ds. \end{aligned} \tag{2.7}$$

Substituting (2.6) and (2.7) into (2.5) yields

$$\mathbb{E} \left[ \sup_{0 \leq s \leq t} |p_{n+1}(s) - p_n(s)|^2 \right] \leq Q_T \int_0^t \mathbb{E} \left[ \sup_{0 \leq r \leq s} |p_n(r) - p_{n-1}(r)|^2 \right] ds,$$

where  $Q_T = 2T(\sigma^2 Q_0^2 + L)$ .

For any  $n \geq 1$ , we define  $h_n(t)$  by

$$h_n(t) := \mathbb{E} \left[ \sup_{0 \leq s \leq t} |p_{n+1}(s) - p_n(s)|^2 \right].$$

Note that the term  $h_0(t)$  can be estimated as follows:

$$\begin{aligned}
 h_0(t) &:= \mathbb{E} \left[ \sup_{0 \leq s \leq t} |p_1(s) - p_0(s)|^2 \right] \\
 &\leq 3 \mathbb{E} \left[ \sup_{0 \leq s \leq t} \sigma^2 v_0^2 \left( \int_0^t |c_1(t, s)| ds \right)^2 + \sup_{0 \leq s \leq t} \left( \int_0^t |f(v_0)| ds \right)^2 \right. \\
 &\quad \left. + \sup_{0 \leq s \leq t} \left( \int_0^s |c_2(s, r)| d\mathcal{B}(r) \right)^2 \right] \\
 &\leq 3 (\sigma^2 Q_0^2 t^2 \mathbb{E}[v_0^2] + L t^2 (1 + \mathbb{E}[v_0^2]) + Q_1^2 t) \\
 &\leq 3T (\sigma^2 Q_0^2 T + LT) \mathbb{E}[v_0^2] + 3T (LT + Q_1^2) =: Q'_T.
 \end{aligned}$$

Consequently,

$$h_n(t) \leq \frac{Q'_T Q_T^n t^n}{\Gamma(n+1)}, \quad t \in [0, T],$$

and

$$\sum_{n=0}^{\infty} \frac{Q'_T Q_T^n t^n}{\Gamma(n+1)} = Q'_T e^{Q_T t} < \infty, \quad t \in [0, T],$$

which implies

$$\sum_{n=0}^{\infty} \mathbb{E} \left[ \sup_{0 \leq t \leq T} |p_{n+1}(t) - p_n(t)|^2 \right] < \infty.$$

Recalling the Chebyshev inequality, we write

$$\begin{aligned}
 &\mathbb{P} \left( \sup_{t \in [0, T]} |p_{n+1}(t) - p_n(t)| \geq 2^{-n} \right) \\
 &\leq 4^n \mathbb{E} \left[ \sup_{t \in [0, T]} |p_{n+1}(t) - p_n(t)|^2 \right] \leq \frac{4^n Q'_T (Q_T T)^n}{\Gamma(n+1)},
 \end{aligned}$$

and applying the Borel-Cantelli lemma show that

$$p_n(t) = \sum_{m=1}^n (p_m(t) - p_{m-1}(t)) + v_0$$

converges uniformly on  $[0, T]$  to a limit  $v$  that solves (2.1).

Assume  $\tilde{v}$  is a solution other than  $v(x)$ . Then

$$\mathbb{E} \left[ \sup_{0 \leq s \leq t} |v(s) - \tilde{v}(s)|^2 \right] \leq Q_T \int_0^t \mathbb{E} \left[ \sup_{0 \leq r \leq s} |v(r) - \tilde{v}(r)|^2 \right] ds,$$

and we conclude that  $v(s) = \tilde{v}(s)$  a.s.

Applying (2.2), (2.3) and Assumption 2.3, we bound  $\mathbb{E}[\sup_{0 \leq x \leq t} |p_n(x)|^2]$  for  $n \geq 1$  and  $t \in [0, T]$  by

$$\begin{aligned}
\mathbb{E} \left[ \sup_{0 \leq s \leq t} |p_n(s)|^2 \right] &\leq 4\mathbb{E}[v_0^2] + 4\sigma^2 \mathbb{E} \left[ \sup_{0 \leq s \leq t} \left( \int_0^s c_1(s, r) p_{n-1}(r) dr \right)^2 \right] \\
&\quad + 4\mathbb{E} \left[ \sup_{0 \leq s \leq t} \left( \int_0^s f(p_{n-1}(r)) dr \right)^2 \right] \\
&\quad + 4\mathbb{E} \left[ \sup_{0 \leq s \leq t} \left( \int_0^s c_2(s, r) dB(r) \right)^2 \right] \\
&\leq 4\mathbb{E}[v_0^2] + 4TQ_0^2\sigma^2 \int_0^t \mathbb{E} \left[ \sup_{0 \leq r \leq s} |p_{n-1}(r)|^2 \right] ds \\
&\quad + 4LT^2 + 4LT \int_0^t \mathbb{E} \left[ \sup_{0 \leq r \leq s} |p_{n-1}(r)|^2 \right] ds + 4TQ_1^2 \\
&= Q_2 + Q_3 \int_0^t \mathbb{E} \left[ \sup_{0 \leq r \leq s} |p_{n-1}(r)|^2 \right] ds,
\end{aligned}$$

where  $Q_2, Q_3$  are defined in (2.4). Invoking the Gronwall inequality yields the proof.  $\square$

### 3. Numerical Discretization and Error Estimate

We develop an Euler-Maruyama scheme [7, 15] for (2.1) and establish its strong convergence rate under Assumptions 2.1-2.3.

#### 3.1. The numerical scheme

Partition  $[0, T]$  by  $t_n := n\tau$  with  $\tau := T/N$  for  $0 \leq n \leq N$ . We discrete (2.1) by

$$\begin{aligned}
\int_0^{t_n} c_1(t_n, s) v(s) ds &\approx \sum_{l=0}^{n-1} \int_{t_l}^{t_{l+1}} c_1(t_n, t_l) v(t_l) ds = \tau \sum_{l=0}^{n-1} c_1(t_n, t_l) v(t_l), \\
\int_0^{t_n} f(v(s)) ds &\approx \sum_{l=0}^{n-1} \int_{t_l}^{t_{l+1}} f(v(t_l)) ds = \tau \sum_{l=0}^{n-1} f(v(t_l)), \\
\int_0^{t_n} c_2(t_n, s) d\mathcal{B}(s) &\approx \sum_{l=0}^{n-1} \int_{t_l}^{t_{l+1}} c_2(t_n, t_l) d\mathcal{B}(s) = \sum_{l=0}^{n-1} c_2(t_n, t_l) \Delta \mathcal{B}_l,
\end{aligned}$$

where

$$\Delta \mathcal{B}_l := \mathcal{B}(t_{l+1}) - \mathcal{B}(t_l) \sim N(0, \tau)$$

denotes the Gaussian distribution. Then we have

$$\vartheta_n = v_0 - \sigma \tau \sum_{l=0}^{n-1} c_1(t_n, t_l) \vartheta_l + \tau \sum_{l=0}^{n-1} f(\vartheta_l) + \sum_{l=0}^{n-1} c_2(t_n, t_l) \Delta \mathcal{B}_l. \quad (3.1)$$

**Theorem 3.1.** *The solution  $\vartheta_n$ ,  $1 \leq n \leq N$  in (3.1) satisfies*

$$\mathbb{E}[\vartheta_n^2] \leq Q_4 \exp(Q_5) =: M_1, \quad (3.2)$$

here the constants  $Q_4$  and  $Q_5$  are given by

$$Q_4 = 4\mathbb{E}[v_0^2] + 4T(LT + Q_1^2), \quad Q_5 = 4T(T\sigma^2Q_0^2 + LT).$$

*Proof.* We bound  $\mathbb{E}[\vartheta_n^2]$  by Jensen inequality,

$$\begin{aligned} \mathbb{E}[\vartheta_n^2] &\leq 4\mathbb{E}[v_0^2] + 4\sigma^2\tau^2\mathbb{E}\left[\left(\sum_{l=0}^{n-1}c_1(t_n, t_l)\vartheta_l\right)^2\right] \\ &\quad + 4\tau^2\mathbb{E}\left[\left(\sum_{l=0}^{n-1}f(\vartheta_l)\right)^2\right] + 4\mathbb{E}\left[\left(\sum_{l=0}^{n-1}c_2(t_n, t_l)\Delta\mathcal{B}_l\right)^2\right]. \end{aligned} \quad (3.3)$$

Utilizing (2.2), (2.3), Assumption 2.3 and Itô isometry yields

$$4\sigma^2\tau^2\mathbb{E}\left[\left(\sum_{l=0}^{n-1}c_1(t_n, t_l)\vartheta_l\right)^2\right] \leq 4\sigma^2Q_0^2T\tau\sum_{l=0}^{n-1}\mathbb{E}[\vartheta_l^2], \quad (3.4)$$

$$4\tau^2\mathbb{E}\left[\left(\sum_{l=0}^{n-1}f(\vartheta_l)\right)^2\right] \leq 4LT^2 + 4LT\tau\sum_{l=0}^{n-1}\mathbb{E}[\vartheta_l^2], \quad (3.5)$$

$$4\mathbb{E}\left[\left(\sum_{l=0}^{n-1}c_2(t_n, t_l)\Delta\mathcal{B}_l\right)^2\right] \leq 4TQ_1^2. \quad (3.6)$$

Incorporating (3.4)-(3.6) into (3.3), we obtain

$$\mathbb{E}[\vartheta_n^2] \leq Q_4 + \frac{Q_5}{N}\sum_{l=0}^{n-1}\mathbb{E}[\vartheta_l^2].$$

Applying the discrete Gronwall's inequality to obtain (3.2).  $\square$

### 3.2. Error estimates

Using step function  $\hat{s} = \hat{s}(s)$  to define an auxiliary continuous time stochastic process  $\vartheta(t)$  on  $[0, T]$  such that

$$\vartheta(t) = v(0) - \sigma \int_0^t c_1(t, \hat{s})\vartheta(\hat{s})ds + \int_0^t f(\vartheta(\hat{s}))ds + \int_0^t c_2(t, \hat{s})d\mathcal{B}(s), \quad (3.7)$$

where  $\hat{s}(s) = t_n$  when  $s \in [t_n, t_{n+1})$ . It is easy to show that  $\vartheta(t_n) = \vartheta_n$ .

**Lemma 3.1.** Let  $q \in (0, 1]$ . For any nonnegative real numbers  $x$  and  $y$  with  $x < y$ ,

$$y^q - x^q \leq (y - x)^q.$$

Equality holds if and only if  $q = 1$  or  $x = 0$ .

*Proof.* Since  $q \in (0, 1)$ ,  $t^{q-1}$  is non-increasing on  $t \in (0, \infty)$ , for  $x \in (0, \infty)$ , we have

$$y^q - x^q = \int_x^y qs^{q-1} ds \leq \int_x^y q(s-x)^{q-1} ds = (y-x)^q.$$

The proof is complete.  $\square$

**Theorem 3.2.** For  $\vartheta(t)$  defined in (3.7) with  $t \in [t_n, t_{n+1})$ , where  $0 \leq n \leq N-1$ , there exists a constant  $M_2$  independent of  $\tau$  such that

$$\mathbb{E} \left[ (\vartheta(t) - \vartheta(t_n))^2 \right] \leq M_2 \tau^{2 \min\{H(t_n), H(t)\}},$$

where

$$\begin{aligned} M_2 &= 6M_1\sigma^2(Q_6^2 + Q_0^2) + 3L(1 + M_1) \\ &\quad + 12 \left( 10 + Q_8 + 2\zeta(3 - 2H(t_n)) + 8TQ_7\|H\|_{C^1[0,T]}^2 \right), \\ Q_6 &= (\max\{T, 1\}) / (H_{\min} - 0.5), \\ Q_7 &= \left( \max \left\{ \frac{1}{(H_{\min} - 0.5)e}, T^{0.5} \ln T \right\} \right)^2, \\ Q_8 &= 8Q_0T\|H\|_{C^1[0,T]}^2 \max_{s \in [1, 1.5]} \|\Gamma'(s)\|^2, \end{aligned} \tag{3.8}$$

and  $Q_0$  is defined in (2.2),  $M_1$  is defined in (3.2),  $\zeta$  is the riemann's  $\zeta$  function.

*Proof.* Employing Jensen inequality, we write

$$\begin{aligned} \mathbb{E} \left[ (\vartheta(t) - \vartheta(t_n))^2 \right] &\leq 3\sigma^2 \mathbb{E} \left[ \left( \int_0^t c_1(t, \hat{s}) \vartheta(\hat{s}) ds - \int_0^{t_n} c_1(t_n, \hat{s}) \vartheta(\hat{s}) ds \right)^2 \right] \\ &\quad + 3\mathbb{E} \left[ \left( \int_0^t f(v(\hat{s})) ds - \int_0^{t_n} f(v(\hat{s})) ds \right)^2 \right] \\ &\quad + 3\mathbb{E} \left[ \left( \int_0^t c_2(t, \hat{s}) d\mathcal{B}(s) - \int_0^{t_n} c_2(t_n, \hat{s}) d\mathcal{B}(s) \right)^2 \right] \\ &\leq 6\sigma^2 \mathbb{E} \left[ \left( \int_0^{t_n} (c_1(t, \hat{s}) - c_1(t_n, \hat{s})) \vartheta(\hat{s}) ds \right)^2 \right] \\ &\quad + 6\sigma^2 \mathbb{E} \left[ \left( \int_{t_n}^t c_1(t, \hat{s}) \vartheta(\hat{s}) ds \right)^2 \right] + 3\mathbb{E} \left[ \left( \int_{t_n}^t f(v(\hat{s})) ds \right)^2 \right] \end{aligned}$$

$$\begin{aligned}
 & + 6\mathbb{E} \left[ \left( \int_0^{t_n} (c_2(t, \hat{s}) - c_2(t_n, \hat{s})) d\mathcal{B}(s) \right)^2 \right] \\
 & + 6\mathbb{E} \left[ \left( \int_{t_n}^t c_2(t, \hat{s}) d\mathcal{B}(s) \right)^2 \right].
 \end{aligned} \tag{3.9}$$

Using the Cauchy inequality and Theorem 3.1, we write

$$\begin{aligned}
 & 6\sigma^2 \mathbb{E} \left[ \left( \int_0^{t_n} (c_1(t, \hat{s}) - c_1(t_n, \hat{s})) \vartheta(\hat{s}) ds \right)^2 \right] \\
 & \leq 6\sigma^2 \left( \int_0^{t_n} |c_1(t, \hat{s}) - c_1(t_n, \hat{s})| ds \int_0^{t_n} |c_1(t, \hat{s}) - c_1(t_n, \hat{s})| \mathbb{E} [\vartheta(\hat{s})^2] ds \right) \\
 & = 6\sigma^2 \mathbb{E} [\vartheta(\hat{s})^2] \left( \int_0^{t_n} |c_1(t, \hat{s}) - c_1(t_n, \hat{s})| ds \right)^2 \\
 & \leq 6M_1\sigma^2 \left( \int_0^{t_n} |c_1(t, \hat{s}) - c_1(t_n, \hat{s})| ds \right)^2 \leq 6M_1\sigma^2 Q_6^2 \tau^2.
 \end{aligned} \tag{3.10}$$

It follows from the mean value theorem that

$$\begin{aligned}
 & \int_0^{t_n} |c_1(t, \hat{s}) - c_1(t_n, \hat{s})| ds \\
 & = \sum_{l=0}^{n-1} \int_{t_l}^{t_{l+1}} \frac{1}{\Gamma(2H(t_l))} [(t - t_l)^{2H(t_l)-1} - (t_n - t_l)^{2H(t_l)-1}] ds \\
 & \leq \tau \sum_{l=0}^{n-1} \frac{2H(t_l) - 1}{\Gamma(2H(t_l))} \int_{t_l}^{t_{l+1}} (t_n - t_l)^{2H(t_l)-2} ds \\
 & \leq 2\tau^2 \sum_{l=0}^{n-1} (t_n - t_l)^{2H(t_l)-2} \leq \frac{\max\{T, 1\}}{H_{\min} - 0.5} \tau = Q_6 \tau.
 \end{aligned}$$

Using the Cauchy inequality and (3.2) yields

$$6\sigma^2 \mathbb{E} \left[ \left( \int_{t_n}^t c_1(t, \hat{s}) \vartheta(\hat{s}) ds \right)^2 \right] \leq 6M_1\sigma^2 \tau \int_{t_n}^t |c_1(t, \hat{s})|^2 ds \leq 6M_1\sigma^2 Q_0^2 \tau^2. \tag{3.11}$$

We then apply Assumption 2.3, Cauchy inequality and (3.2) to obtain

$$3\mathbb{E} \left[ \left( \int_{t_n}^t f(\vartheta(\hat{s})) ds \right)^2 \right] \leq 3L\tau \int_{t_n}^t (1 + \mathbb{E} [|\vartheta_n|^2]) ds \leq 3L(1 + M_1)\tau^2. \tag{3.12}$$

Using the Cauchy' inequality, Itô isometry, and (3.2) gives

$$\begin{aligned}
& 6\mathbb{E}\left[\left(\int_0^{t_n} (c_2(t, \hat{s}) - c_2(t_n, \hat{s}))d\mathcal{B}(s)\right)^2\right] \\
&= 6\int_0^{t_n} \left(\frac{(t-\hat{s})^{H(t)-0.5}}{\Gamma(H(t)+0.5)} - \frac{(t_n-\hat{s})^{H(t_n)-0.5}}{\Gamma(H(t_n)+0.5)}\right)^2 ds \\
&= 6\int_0^{t_n} \left(\frac{(t-\hat{s})^{H(t)-0.5} - (t_n-\hat{s})^{H(t_n)-0.5}}{\Gamma(H(t)+0.5)}\right. \\
&\quad \left.+ ((t_n-\hat{s})^{H(t_n)-0.5})\left(\frac{1}{\Gamma(H(t)+0.5)} - \frac{1}{\Gamma(H(t_n)+0.5)}\right)\right)^2 ds \\
&\leq 12\left(\int_0^{t_n} \left(\frac{(t-\hat{s})^{H(t)-0.5} - (t_n-\hat{s})^{H(t_n)-0.5}}{\Gamma(H(t)+0.5)}\right)^2 ds\right. \\
&\quad \left.+ \int_0^{t_n} (t_n-\hat{s})^{2H(t_n)-1} \left(\frac{1}{\Gamma(H(t)+0.5)} - \frac{1}{\Gamma(H(t_n)+0.5)}\right)^2 ds\right) \\
&=: 12(J_1 + J_2). \tag{3.13}
\end{aligned}$$

Let  $l \in (t_n, t)$ . Using mean value theorem and Lemma 3.1, we evaluate  $J_1$  as

$$\begin{aligned}
J_1 &= \int_0^{t_n} \left(\frac{(t-\hat{s})^{H(t)-0.5} - (t_n-\hat{s})^{H(t_n)-0.5}}{\Gamma(H(t)+0.5)}\right)^2 ds \\
&\leq 8\int_0^{t_n} \left((t-\hat{s})^{H(t)-0.5} - (t-\hat{s})^{H(t_n)-0.5}\right)^2 \\
&\quad + \left((t-\hat{s})^{H(t_n)-0.5} - (t_n-\hat{s})^{H(t_n)-0.5}\right)^2 ds \\
&\leq 8\|H\|_{C_1[0,T]}^2 \tau^2 \int_0^{t_n} |(t-\hat{s})^{H(l)-0.5} \ln(t-\hat{s})|^2 ds \\
&\quad + 8\int_0^{t_n} ((H(t_n)-0.5)(t_n-\hat{s})^{H(t_n)-1.5} \tau)^2 ds \\
&= 8\|H\|_{C_1[0,T]}^2 \tau^2 \int_0^{t_n} \max_{l \in [t_n, t]} |(t-\hat{s})^{H(l)-0.5} \ln(t-\hat{s})|^2 ds \\
&\quad + 2\tau^2 \left(\sum_{l=0}^{n-1} \int_{t_l}^{t_{l+1}} (t_n - t_l)^{2H(t_n)-3} ds\right) \\
&\leq (8 + 2\zeta(3 - 2H(t_n)))\tau^{2H(t_n)} + 8TQ_7\|H\|_{C_1[0,T]}^2 \tau^2,
\end{aligned}$$

since

$$\max_{l \in [t_n, t]} |(t-\hat{s})^{H(l)-0.5} \ln(t-\hat{s})|^2 \leq \left(\max\left\{\frac{1}{(H_{\min}-0.5)e}, T^{0.5} \ln T\right\}\right)^2 = Q_7,$$

and

$$\sum_{l=0}^{n-1} \int_{t_l}^{t_{l+1}} (t_n - t_l)^{2H(t_n)-3} ds = \tau^{2H(t_n)-2} \sum_{i=1}^{n-1} i^{2H(t_n)-3} \leq \tau^{2H(t_n)-2} \zeta(3 - 2H(t_n)).$$

Besides, we bound  $J_2$  by

$$\begin{aligned} J_2 &= \int_0^{t_n} ((t_n - \hat{s})^{H(t_n)-0.5})^2 \left( \frac{1}{\Gamma(H(t) + 0.5)} - \frac{1}{\Gamma(H(t_n) + 0.5)} \right)^2 ds \\ &\leq \left( \frac{\Gamma(H(t_n) + 0.5) - \Gamma(H(t) + 0.5)}{\Gamma(H(t_n) + 0.5)\Gamma(H(t) + 0.5)} \right)^2 \int_0^{t_n} (t_n - \hat{s})^{2H(t_n)-1} ds \leq Q_8 \tau^2 \end{aligned}$$

with  $Q_8$  introduced in (3.8). Using Itô isometry, we have

$$\begin{aligned} &6\mathbb{E} \left[ \left( \int_{t_n}^t c_2(t, \hat{s}) d\mathcal{B}(s) \right)^2 \right] \\ &= 6 \int_{t_n}^t (c_2(t, \hat{s}))^2 ds = 6 \int_{t_n}^t \frac{(t - t_n)^{2H(t)-1}}{\Gamma^2(H(t) + 0.5)} ds \leq 24\tau^{2H(t)}. \end{aligned} \quad (3.14)$$

Substituting (3.10)-(3.14) into (3.9) finishes the proof.  $\square$

Before we obtain Theorem 3.3, we need following lemmas.

**Lemma 3.2.** *Under Assumption 2.1, for  $t \in [t_n, t_{n+1}]$ , it holds*

$$\int_0^t |c_1(t, s) - c_1(t, \hat{s})| ds \leq M_3 \tau,$$

where

$$M_3 := 4T \|H\|_{C^1[0, T]} \max_{1 \leq t \leq 2} |\Gamma'(t)| Q_0 + 2 \left( \frac{1}{2H_{\min} - 1} + \frac{T^{2H_{\max} - 1}}{2H_{\max} - 1} + 2Q_7 \|H\|_{C^1[0, T]} \right).$$

*Proof.* First, we write

$$\begin{aligned} &\int_0^t |c_1(t, s) - c_1(t, \hat{s})| ds \\ &= \int_0^t \left| \frac{(t-s)^{2H(s)-1}}{\Gamma(2H(s))} - \frac{(t-s)^{2H(s)-1}}{\Gamma(2H(\hat{s}))} + \frac{(t-s)^{2H(s)-1}}{\Gamma(2H(\hat{s}))} - \frac{(t-\hat{s})^{2H(\hat{s})-1}}{\Gamma(2H(\hat{s}))} \right| ds \\ &\leq \int_0^t \left| \frac{\Gamma(2H(\hat{s})) - \Gamma(2H(s))}{\Gamma(2H(s))\Gamma(2H(\hat{s}))} (t-s)^{2H(s)-1} \right| ds \\ &\quad + \int_0^t \left| \frac{(t-s)^{2H(s)-1} - (t-\hat{s})^{2H(\hat{s})-1}}{\Gamma(2H(\hat{s}))} \right| ds \\ &=: J_3 + J_4, \end{aligned} \quad (3.15)$$

and bound  $J_3$  as

$$J_3 \leq 4T \|H\|_{C^1[0,T]} \max_{1 \leq t \leq 2} |\Gamma'(t)| Q_0 \tau. \quad (3.16)$$

Now we split  $J_4$  into two parts,

$$\begin{aligned} J_4 &\leq 2 \int_0^t |(t-s)^{2H(s)-1} - (t-\hat{s})^{2H(s)-1}| ds \\ &\quad + 2 \int_0^t |(t-\hat{s})^{2H(s)-1} - (t-\hat{s})^{2H(\hat{s})-1}| ds \\ &=: 2J_{4,1} + 2J_{4,2}. \end{aligned} \quad (3.17)$$

By the mean value theorem, the term  $J_{4,1}$  can be evaluated as

$$\begin{aligned} J_{4,1} &= \int_0^t |(t-s)^{2H(s)-1} - (t-\hat{s})^{2H(s)-1}| ds \\ &\leq \tau \int_0^t (t-s)^{2H(s)-2} ds \leq \left( \frac{1}{2H_{\min}-1} + \frac{T^{2H_{\max}-1}}{2H_{\max}-1} \right) \tau. \end{aligned} \quad (3.18)$$

For the term  $J_{4,2}$ , we have

$$J_{4,2} \leq 2 \|H\|_{C^1[0,T]} \tau \int_0^t \max_{\hat{s} \leq l \leq s} |(t-\hat{s})^{2H(l)-1} \ln(t-\hat{s})| ds \leq 2Q_7 \|H\|_{C^1[0,T]} \tau, \quad (3.19)$$

where  $Q_7$  is defined in (3.8). Combining (3.15)-(3.19) finishes the proof.  $\square$

**Lemma 3.3.** *Under Assumption 2.1, for  $t \in [t_n, t_{n+1}]$ , it holds*

$$\int_0^t (c_2(t,s) - c_2(t,\hat{s}))^2 ds \leq Q_8 \tau^{2H(t)},$$

where

$$Q_8 = \frac{2}{3(1-H_{\max})} + 16.$$

*Proof.* We have

$$\begin{aligned} &\int_0^t (c_2(t,s) - c_2(t,\hat{s}))^2 ds \\ &= \int_0^t \left( \frac{(t-s)^{H(t)-0.5}}{\Gamma(H(t)+0.5)} - \frac{(t-\hat{s})^{H(t)-0.5}}{\Gamma(H(t)+0.5)} \right)^2 ds \\ &\leq 4 \left( \sum_{l=0}^{n-2} \int_{t_l}^{t_{l+1}} ((t-s)^{H(t)-0.5} - (t-t_l)^{H(t)-0.5})^2 ds + \int_{t_{n-1}}^t (s-t_{n-1})^{2H(t)-1} ds \right) \end{aligned}$$

$$\begin{aligned}
 &\leq 4 \sum_{l=0}^{n-2} \int_0^\tau \left( (t-t_l-u)^{H(t)-0.5} - (t-t_l)^{H(t)-0.5} \right)^2 du + \frac{2^{2H(t)+1}}{H(t)} \tau^{2H(t)} \\
 &\leq 4 \sum_{l=0}^{n-2} (t-t_l)^{2H(t)-1} \int_0^\tau \left( \left( 1 - \frac{u}{t-t_l} \right)^{H(t)-0.5} - 1 \right)^2 du + \frac{2^{2H(t)+1}}{H(t)} \tau^{2H(t)} \\
 &\leq 4 \sum_{l=0}^{n-2} (t-t_l)^{2H(t)-3} \int_0^\tau u^2 du + \frac{2^{2H(t)+1}}{H(t)} \tau^{2H(t)} \\
 &\leq \frac{4\tau^3}{3} \sum_{l=0}^{n-2} (t-t_l)^{2H(t)-3} + \frac{2^{2H(t)+1}}{H(t)} \tau^{2H(t)} \\
 &\leq \left( \frac{2}{3(1-H_{\max})} + 16 \right) \tau^{2H(t)} = Q_8 \tau^{2H(t)},
 \end{aligned}$$

and the proof is complete.  $\square$

**Theorem 3.3.** *Let  $v$  and  $y$  be the solutions to models (2.1) and (3.7), respectively. Under Assumptions 2.1-2.3, we have the following estimate:*

$$\mathbb{E}[|v(t) - \vartheta(t)|^2] \leq Q_{10}(Q_{12}\tau^{2H_{\min}} + Q_{13}\tau^{2H(t)} + Q_{14}\tau^2),$$

where

$$\begin{aligned}
 Q_{10} &= \exp(Q_{11}T), & Q_{12} &= 12Q_0^2T^2\sigma^2M_2 + 6LM_2T^2, \\
 Q_{11} &= 6(2TQ_0^2\sigma^2 + LT), & Q_{13} &= 3Q_8, & Q_{14} &= 12M_1M_3^2\sigma^2.
 \end{aligned}$$

In particular, if  $\vartheta(t_n) = \vartheta_n$ , then

$$\mathbb{E}[|v(t_n) - \vartheta_n|^2] \leq Q_{10}(Q_{12}\tau^{2H_{\min}} + Q_{13}\tau^{2H(t_n)} + Q_{14}\tau^2).$$

*Proof.* Applying the Jensen inequality gives

$$\begin{aligned}
 \mathbb{E}[|v(t) - \vartheta(t)|^2] &\leq 3\sigma^2 \mathbb{E} \left[ \left( \int_0^t c_1(t,s)v(s) - c_1(t,\hat{s})\vartheta(\hat{s})ds \right)^2 \right] \\
 &\quad + 3\mathbb{E} \left[ \left( \int_0^t f(v(s)) - f(\vartheta(\hat{s}))ds \right)^2 \right] \\
 &\quad + 3\mathbb{E} \left[ \left( \int_0^t c_2(t,s) - c_2(t,\hat{s})d\mathcal{B}(s) \right)^2 \right] \\
 &=: I_1 + I_2 + I_3.
 \end{aligned}$$

We bound  $I_1$  by

$$3\sigma^2 \mathbb{E} \left[ \left( \int_0^t c_1(t,s)v(s) - c_1(t,\hat{s})\vartheta(\hat{s})ds \right)^2 \right]$$

$$\begin{aligned}
&= 3\sigma^2 \mathbb{E} \left[ \left( \int_0^t c_1(t,s)v(s) - c_1(t,s)\vartheta(\hat{s}) + c_1(t,s)\vartheta(\hat{s}) - c_1(t,\hat{s})\vartheta(\hat{s}) ds \right)^2 \right] \\
&\leq 6\sigma^2 \mathbb{E} \left[ \left( \int_0^t c_1(t,s)(v(s) - \vartheta(\hat{s})) ds \right)^2 \right] + 6\sigma^2 \mathbb{E} \left[ \left( \int_0^t (c_1(t,s) - c_1(t,\hat{s}))\vartheta(\hat{s}) ds \right)^2 \right] \\
&=: I_{1,1} + I_{1,2}.
\end{aligned}$$

Taking into account Theorem 3.2 and Lemma 3.2, we write

$$\begin{aligned}
I_{1,1} &= 6\sigma^2 \mathbb{E} \left[ \left( \int_0^t c_1(t,s)(v(s) - \vartheta(s) + \vartheta(s) - \vartheta(\hat{s})) ds \right)^2 \right] \\
&\leq 12TQ_0^2\sigma^2 \int_0^t \mathbb{E} [(v(s) - \vartheta(s))^2] ds + 12\sigma^2 \mathbb{E} \left[ \left( \int_0^t c_1(t,s)(\vartheta(s) - \vartheta(\hat{s})) ds \right)^2 \right] \\
&\leq 12TQ_0^2\sigma^2 \int_0^t \mathbb{E} [(v(s) - \vartheta(s))^2] ds + 12Q_0^2T^2\sigma^2M_2\tau^{2H_{\min}},
\end{aligned}$$

where

$$\begin{aligned}
&\int_0^t \mathbb{E} [(\vartheta(s) - \vartheta(\hat{s}))^2] ds \\
&\leq \sum_{l=0}^{n-1} \int_{t_l}^{t_{l+1}} \mathbb{E} [(\vartheta(s) - \vartheta(t_l))^2] ds \\
&\leq M_2 \sum_{l=0}^{n-1} \int_{t_l}^{t_{l+1}} \tau^{2\min\{H(t_l), H(s)\}} ds \leq M_2\tau^{2H_{\min}}. \tag{3.20}
\end{aligned}$$

In addition, the term  $I_{1,2}$  admits the estimate

$$\begin{aligned}
I_{1,2} &= 6\sigma^2 \mathbb{E} \left[ \left( \int_0^t (c_1(t,s) - c_1(t,\hat{s}))\vartheta(\hat{s}) ds \right)^2 \right] \\
&\leq 6\sigma^2 \mathbb{E} \left[ \int_0^t (c_1(t,s) - c_1(t,\hat{s})) ds \int_0^t (c_1(t,s) - c_1(t,\hat{s}))\vartheta(\hat{s})^2 ds \right] \\
&\leq 6M_1\sigma^2 \left( \int_0^t (c_1(t,s) - c_1(t,\hat{s})) ds \right)^2 \leq 12M_1M_3^2\sigma^2\tau^2.
\end{aligned}$$

We bound  $I_2$  by

$$\begin{aligned}
I_2 &= 3\mathbb{E} \left[ \left( \int_0^t f(v(s)) - f(\vartheta(\hat{s})) ds \right)^2 \right] \\
&\leq 3LT \int_0^t \mathbb{E} [|v(s) - \vartheta(\hat{s})|^2] ds
\end{aligned}$$

$$\leq 6LT \int_0^t \mathbb{E}[|v(s) - \vartheta(s)|^2] ds + 6LM_2 T^2 \tau^{2H_{\min}}.$$

Utilizing the Itô isometry and Lemma 3.3 gives

$$I_3 = 3 \int_0^t (c_2(t, s) - c_2(t, \hat{s}))^2 ds \leq 3Q_8 \tau^{2H(t)}.$$

Consequently, we have

$$\mathbb{E}[|v(t) - \vartheta(t)|^2] ds \leq Q_{12} \tau^{2H_{\min}} + Q_{13} \tau^{2H(t)} + Q_{14} \tau^2 + Q_{11} \int_0^t \mathbb{E}[|v(s) - \vartheta(s)|^2] ds.$$

The application of the Gronwall inequality finishes the proof.  $\square$

**Remark 3.1.** Since  $H_{\min} \leq H(t) < 2$ , Theorem 3.3 indicates that, as the partition becomes sufficiently fine, the convergence rate of the error should be  $\mathcal{O}(\tau^{H_{\min}})$  for the scheme (3.1). Nevertheless, this estimate can be conservative in practice. As indicated by the error expression in (3.20), the actual convergence behavior depends more intricately on the functional values  $H(t)$  over the entire interval  $[0, T]$  rather than solely on its minimum. Numerical experiments suggest that the effective convergence rate often exceeds  $H_{\min}$  and aligns more closely with a certain averaged value of  $H(t)$  across the temporal domain.

#### 4. Numerical Simulations

We consider a few examples to validate the foregoing results. The convergence rate of the scheme (3.1) is tested similar to [25]. Let  $j$ -th be a sample path of the numerical approximation computed by (3.1) for  $n = 0, 1, \dots, N$  and  $j = 1, 2, \dots, M$ . In this section, we choose  $\sigma = 0.1$ ,  $v_0 = 1$ ,  $[0, T] = [0, 1]$ ,  $f(v) = \sin^2(v)$  in the VFLE (2.1). The error is evaluated as follows:

$$e_\tau := \left[ \frac{1}{M} \sum_{j=1}^M |\vartheta_{(\tau, N)}(\omega_j) - \vartheta_{(\tau/2, 2N)}(\omega_j)|^2 \right]^{1/2}. \quad (4.1)$$

**Example 4.1.** In this example, we present errors and strong convergence rate for mesh size  $N = 2^2, 2^3, \dots, 2^7$ . We use three distinct sets of time-dependent Hurst index functions  $H(t)$ . The first set consists of a quadratic function

$$H_1(t) = 0.72 - 0.15(t - 0.5)^2,$$

its value ranges from 0.6825 to 0.72 as  $t \in (0, T)$ , a sigmoid function

$$H_2(t) = 0.68 + 0.04/(1 + \exp(-10(t - 0.5))),$$

which increases smoothly from about 0.68 to 0.72, and a periodic function

$$H_3(t) = 0.7 + 0.02 \sin(4\pi t)$$

oscillating between 0.68 and 0.72. The second set consists of a quadratic function

$$H_1(t) = 0.6 + 0.2t^2,$$

a sigmoid function

$$H_2(t) = 0.6 + 0.2/(1 + \exp(-10(t - 0.5))),$$

and a periodic function

$$H_3(t) = 0.7 + 0.1 \sin(2.5\pi t),$$

all of which satisfy  $H(T) = 0.8$  at the terminal time  $T = 1$ , as illustrated in Fig. 5. The second set includes a quadratic function

$$H_1(t) = 0.9 - 0.2(2t - 1)^2,$$

a modified sigmoid function

$$H_2(t) = 0.8 - 0.1 \tanh(5(t - 0.5)),$$

and a weighted periodic function

$$H_3(t) = 0.8 + 0.2 \sin(2\pi t)(1 - t)^{1.5} - 0.1t,$$

which yield  $H(T) = 0.7$  at  $T = 1$ , as shown in Fig. 7. To compute the error (4.1), the total number of independent sample paths  $M = 1000$ .

Numerical convergence results for both sets are displayed in Figs. 4, 6 and 8. The log-log plots demonstrate the relationship between the error and the mesh size. In each plot, the dashed line shows a reference slope in the log-log plot. Its negative slope can be interpreted as an empirical convergence rate and is included only for comparison with the numerically observed error decay, while the solid line with circle markers represents the numerical results obtained for different  $H(t)$  functions plotted in Figs. 3, 5 and 7. For the three types of  $H(t)$  illustrated in Fig. 3, where the function values remain close to 0.7, the observed convergence rates shown in Fig. 4 are approximately 0.7. For the cases presented in Fig. 5, where  $H(T) = 0.8$ , the convergence rates inferred from Fig. 6 approach 0.8. Moreover, for the functions displayed in Fig. 7 whose minimum value equals 0.7, the convergence rates extracted from Fig. 8 are around 0.7. These numerical observations are in agreement with the theoretical error bound established in Theorem 3.3 and support the analysis provided in Remark 3.1.

In Fig. 9, we present three sample paths and the Monte Carlo mean with  $M = 1000$  of the velocity process  $v(t)$ ,

$$\mathbb{E}[v(t)] \approx \frac{1}{M} \sum_{m=1}^M v^{(m)}(t),$$

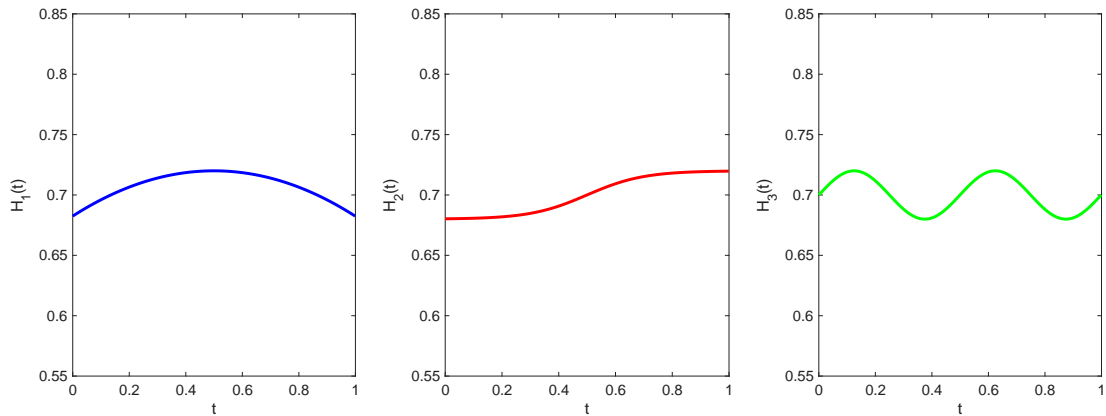


Figure 3: Three types of  $H(t)$  functions. Left:  $H_1(t) = 0.72 - 0.15(t - 0.5)^2$ . Middle:  $H_2(t) = 0.68 + 0.04/(1 + \exp(-10(t - 0.5)))$ . Right:  $H_3(t) = 0.7 + 0.02 \sin(4\pi t)$ .

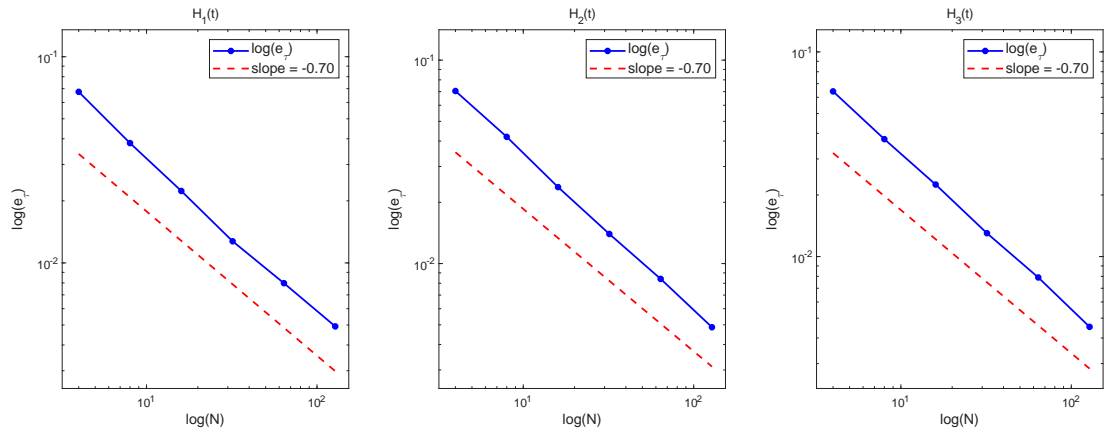


Figure 4: Log-log plots of numerical convergence for the VFLE. Left:  $H_1(t) = 0.72 - 0.15(t - 0.5)^2$ . Middle:  $H_2(t) = 0.68 + 0.04/(1 + \exp(-10(t - 0.5)))$ . Right:  $H_3(t) = 0.7 + 0.02 \sin(4\pi t)$ .

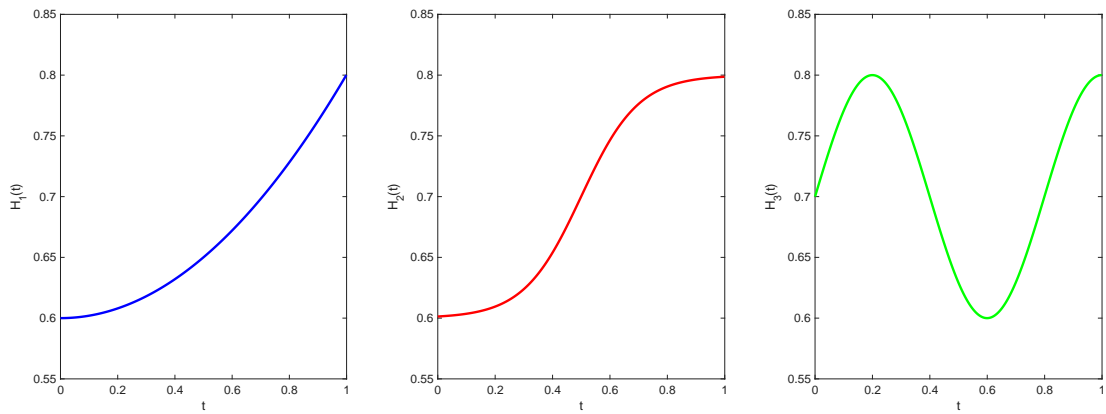


Figure 5: Three types of  $H(t)$  functions. Left:  $H_1(t) = 0.6 + 0.2t^2$ . Middle:  $H_2(t) = 0.6 + 0.2/(1 + \exp(-10(t - 0.5)))$ . Right:  $H_3(t) = 0.7 + 0.1 \sin(2.5\pi t)$ .

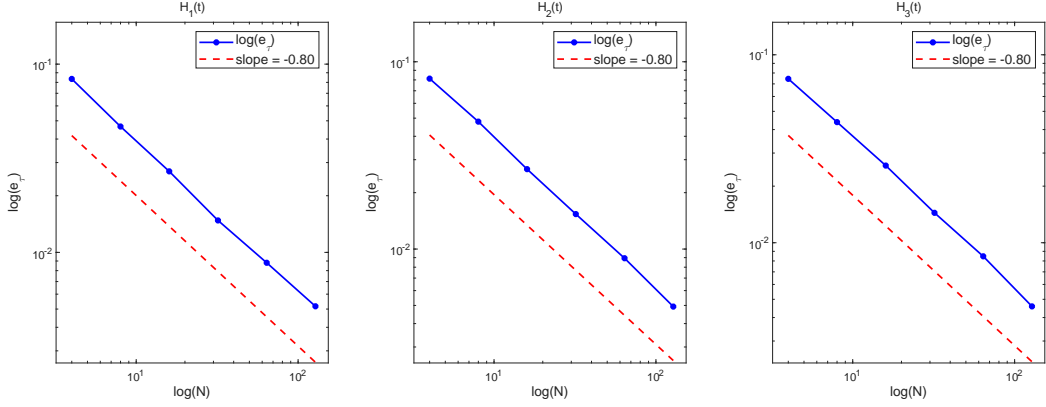


Figure 6: Log-log plots of numerical convergence for the VFLE. Left:  $H_1(t) = 0.6 + 0.2t^2$ . Middle:  $H_2(t) = 0.6 + 0.2/(1 + \exp(-10(t - 0.5)))$ . Right:  $H_3(t) = 0.7 + 0.1 \sin(2.5\pi t)$ .

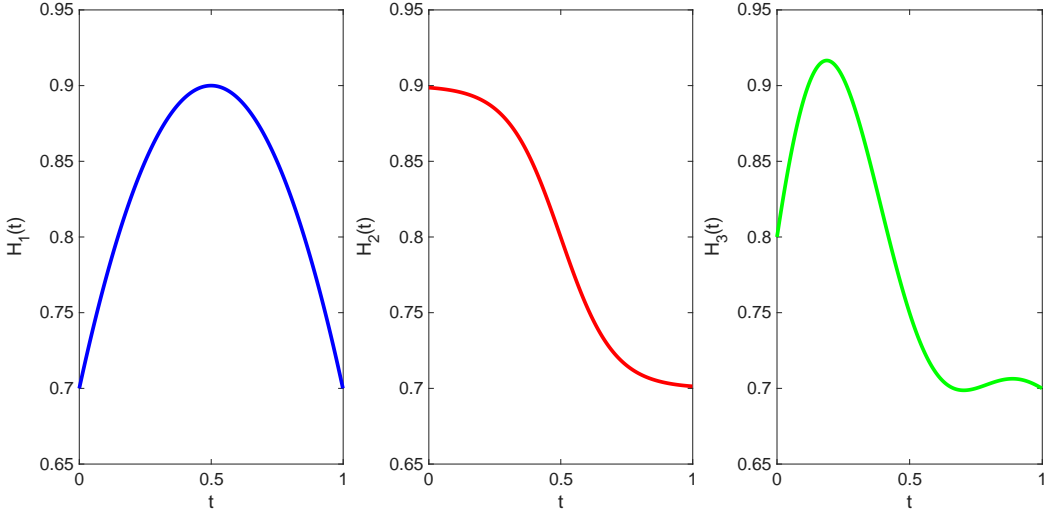


Figure 7: Three types of  $H(t)$  functions. Left:  $H_1(t) = 0.9 - 0.2(2t - 1)^2$ . Middle:  $H_2(t) = 0.8 - 0.1 \tanh(5(t - 0.5))$ . Right:  $H_3(t) = 0.8 + 0.2 \sin(2\pi t)(1 - t)^{1.5} - 0.1t$ .

with Hurst index  $H_1(t) = 0.6 + 0.2t^2$ . The sample paths illustrate the stochastic fluctuations of the process, while the Monte Carlo mean reflects the average behavior. The mean curve shows a clear trend that is smoother than the individual sample paths, indicating the statistical stabilization effect of the averaging procedure.

**Example 4.2.** In this example, we further compute and present the displacement process  $x(t)$  associated with the velocity process  $v(t)$  obtained in Example 4.1, in order to illustrate the full dynamics of the VFLE.

The displacement process  $x(t)$  is recovered from the velocity through the relation  $dx(t) = v(t)dt$ , which is discretized using a forward Euler scheme,

$$x_{n+1} = x_n + \vartheta_n \tau, \quad n = 0, 1, \dots, N - 1.$$

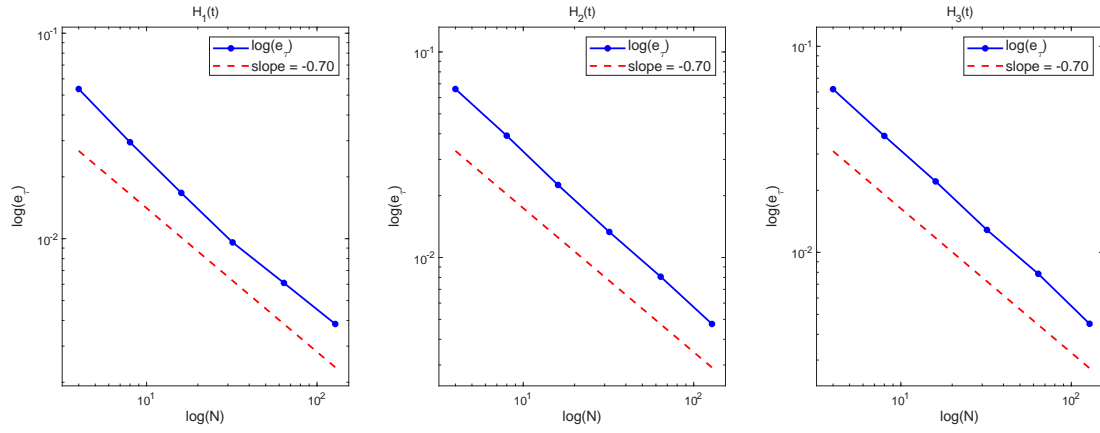


Figure 8: Log-log plots of numerical convergence for the VFLE. Left:  $H_1(t) = 0.9 - 0.2(2t - 1)^2$ . Middle:  $H_2(t) = 0.8 - 0.1 \tanh(5(t - 0.5))$ . Right:  $H_3(t) = 0.8 + 0.2 \sin(2\pi t)(1 - t)^{1.5} - 0.1t$ .

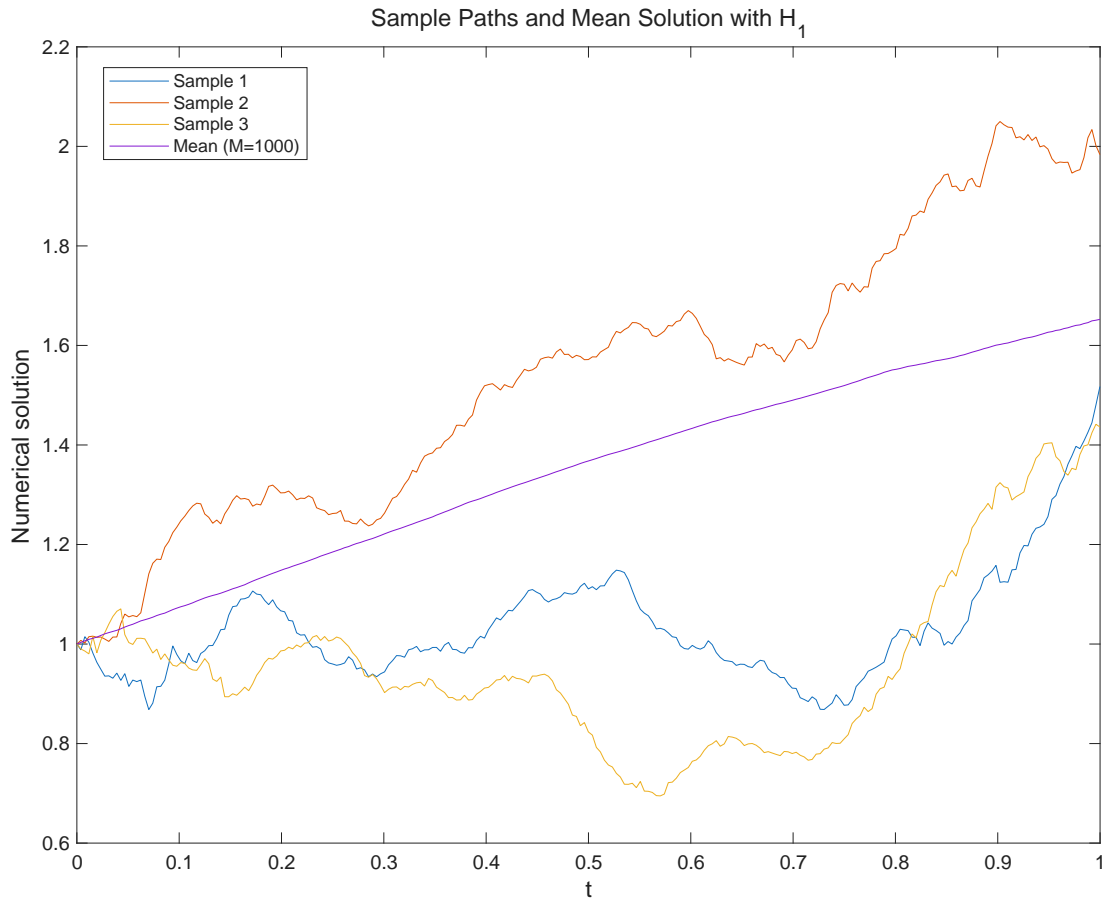
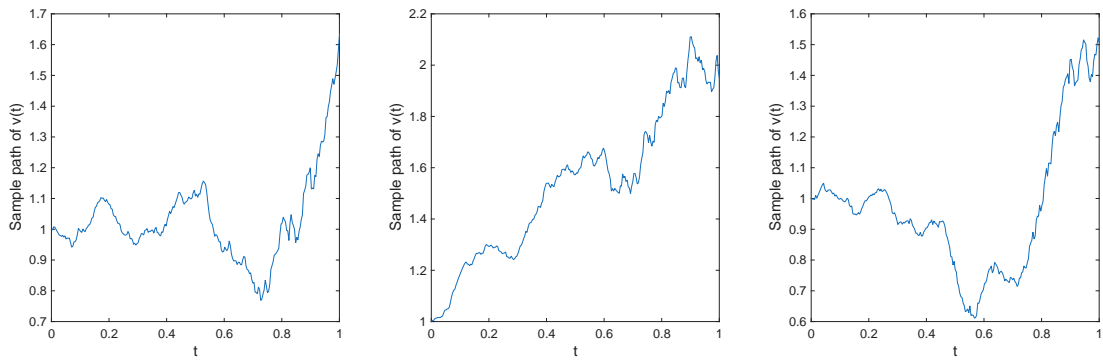
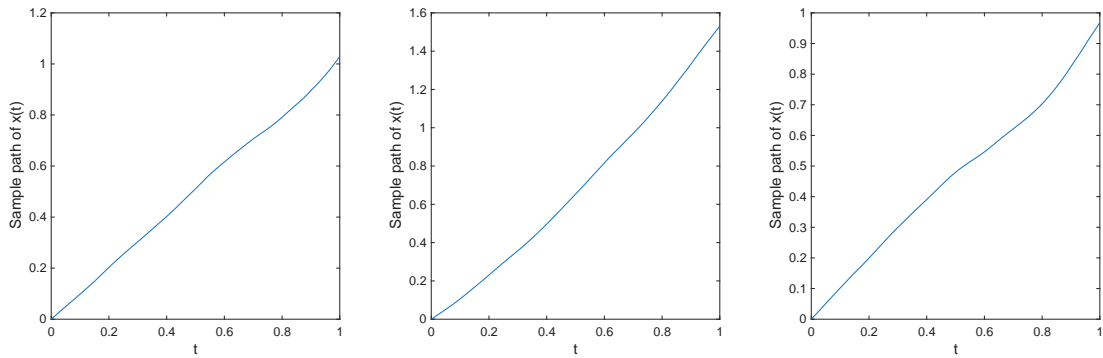
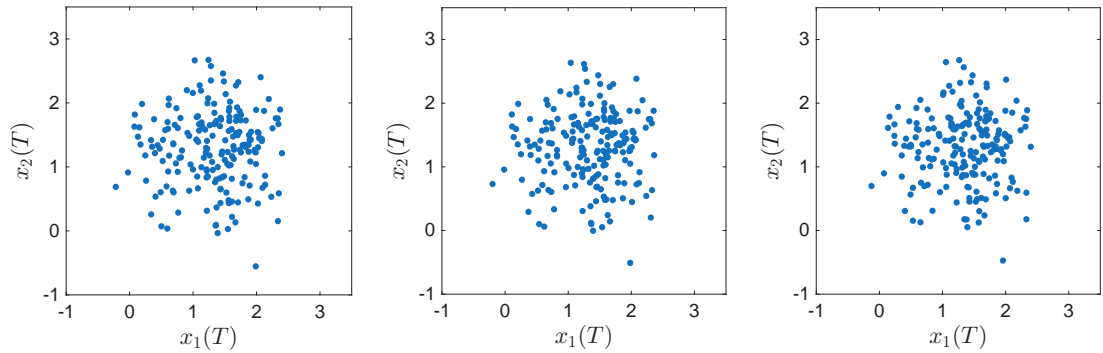


Figure 9: Sample paths and Monte Carlo mean solution for the VFLE with  $H(t) = 0.6 + 0.2t^2$ .

Figure 10: Three independent sample paths of the velocity  $v(t)$ .Figure 11: Three independent sample paths of the displacement  $x(t)$ .Figure 12: Terminal distribution of two-dimensional displacement  $x(T)$  from 200 independent sample paths. Left:  $H_1(t) = 0.6 + 0.2t^2$ . Middle:  $H_2(t) = 0.6 + 0.2/(1 + \exp(-10(t - 0.5)))$ . Right:  $H_3(t) = 0.7 + 0.1 \sin(2.5\pi t)$ .

Figs. 10 and 11 show different sample paths of numerically determined velocity  $\vartheta_n$  and displacement  $x_n$ .

Since the stochastic forcing acts directly on the velocity,  $v(t)$  contains stronger high-frequency fluctuations, while the displacement  $x(t)$ , obtained by time integration of  $v(t)$ , smooths out these oscillations and therefore exhibits much smaller variability.

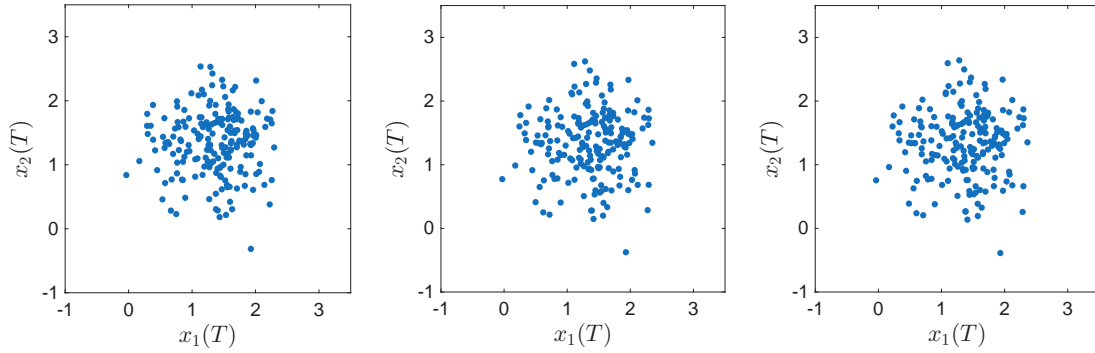


Figure 13: Terminal distribution of two-dimensional displacement  $x(T)$  from 200 independent sample paths. Left:  $H_1(t) = 0.9 - 0.2(2t - 1)^2$ . Middle:  $H_2(t) = 0.8 - 0.1 \tanh(5(t - 0.5))$ . Right:  $H_3(t) = 0.8 + 0.2 \sin(2\pi t)(1 - t)^{1.5} - 0.1t$ .

For the two-dimensional case, Figs. 12 and 13 show the empirical distribution of the terminal displacement  $x(T)$  based on  $M = 200$  independent realizations, unless otherwise stated, all simulations are performed using identical random seeds. The spreading of the point cloud reflects the cumulative memory effect induced by the fractional Langevin dynamics.

A further comparison of Figs. 12 and 13 reveals the clear dependence of the terminal distribution of the displacement  $x(T)$  on the value of the Hurst function near the final time. In Fig. 12, where the Hurst function satisfies  $H(T) = 0.8$ , the terminal distribution is noticeably more spread out than in Fig. 13, which corresponds to a smaller terminal value  $H(T) = 0.7$ .

## 5. Conclusions

This work proposes a variable-order fractional Langevin equation driven by multifractional Brownian motion of Riemann-Liouville type, which describes the long-range interactions. The existence and uniqueness of solutions to the problem are proved. Additionally, an EM scheme for the equation is developed and the corresponding strong convergence of the scheme is proved. Based on the discretization scheme, we conduct the numerical experiments to support our theoretical findings.

## Acknowledgments

The authors would like to express their sincere gratitude to the reviewers for their invaluable comments and suggestions, which have greatly improved the manuscript, as well as to Professor Hong Wang from the University of South Carolina for his invaluable guidance and support throughout this research.

This research was supported by the National Key R&D Program of China (Grant No. 2023YFA1009200), by the National Natural Science Foundation of China (Grant Nos.

12401555, 12131014), by the Natural Science Foundation of Shandong Province of China (Grant No. ZR2025LZN010) and by the Taishan Scholars Program of Shandong Province (Grant No. tsqn202507039). All data generated or analyzed during this study are included in this article.

## References

- [1] J.A. Barnes and D.W. Allan, *A statistical model of flicker noise*, Proc. IEEE **54**, 176–178 (1966).
- [2] M.A. Berger and V.J. Mizel, *Volterra equations with Itô integrals-I*, J. Integral Equ. **2**, 187–245 (1980).
- [3] H. Brunner, *Collocation Methods for Volterra Integral and Related Functional Differential Equations*, Cambridge University Press (2004).
- [4] L.C. Evans, *An Introduction to Stochastic Differential Equations*, AMS (2014).
- [5] D.J. Higham, X. Mao and A.M. Stuart, *Strong convergence of Euler-type methods for nonlinear stochastic differential equations*, SIAM J. Numer. Anal. **40**, 1041–1063 (2002).
- [6] C. Huang and M. Stynes, *Error analysis of a finite element method with GMMP temporal discretization for a time-fractional diffusion equation*, Comput. Math. Appl. **79**, 2784–2794 (2020).
- [7] J. Huang, Z. Huo, J. Zhang and Y. Tang, *An Euler-Maruyama method and its fast implementation for multiterm fractional stochastic differential equations*, Math. Methods Appl. Sci. **46**, 1556–1573 (2023).
- [8] S. Joo and J.-H. Jeon, *Viscoelastic active diffusion governed by nonequilibrium fractional Langevin equations: Underdamped dynamics and ergodicity breaking*, Chaos Solit. Fractals **177**, Paper No. 114288 (2023).
- [9] P.E. Kloeden and E. Platen, *Numerical Solution of Stochastic Differential Equations*, Springer (1992).
- [10] J.-F. Le Gall, *Brownian Motion, Martingales, and Stochastic Calculus*, Springer (2016).
- [11] B. Li, T. Wang and X. Xie, *Analysis of the L1 scheme for fractional wave equations with nonsmooth data*, Comput. Math. Appl. **90**, 1–12 (2021).
- [12] C. Li, D. Li and Z. Wang, *L1/LDG method for the generalized time-fractional Burgers equation in two spatial dimensions*, Commun. Appl. Math. Comput. **5**, 1299–1322 (2023).
- [13] C. Li and Z. Li, *The finite-time blow-up for semilinear fractional diffusion equations with time  $\psi$ -Caputo derivative*, J. Nonlinear Sci. **32**, Paper No. 82 (2022).
- [14] H. Liang and M. Stynes, *Collocation methods for general Riemann-Liouville two-point boundary value problems*, Adv. Comput. Math. **45**, 897–928 (2019).
- [15] H. Liang, Z. Yang and J. Gao, *Strong superconvergence of the Euler-Maruyama method for linear stochastic Volterra integral equations*, J. Comput. Appl. Math. **317**, 447–457 (2017).
- [16] H. Liao, T. Tang and T. Zhou, *An energy stable and maximum bound preserving scheme with variable time steps for time fractional Allen-Cahn equation*, SIAM J. Sci. Comput. **43**, A3503–A3526 (2021).
- [17] G.J. Lord, C.E. Powell and T. Shardlow, *An Introduction to Computational Stochastic PDEs*, Cambridge University Press (2014).
- [18] X. Mao, *Stochastic Differential Equations and Applications*, Elsevier (2007).
- [19] R. Metzler and J. Klafter, *The random walk's guide to anomalous diffusion: A fractional dynamics approach*, Phys. Rep. **339**, 1–77 (2000).
- [20] S.V. Muniandy and S.C. Lim, *Modeling of locally self-similar processes using multifractional Brownian motion of Riemann-Liouville type*, Phys. Rev. E **63**, Paper No. 046104 (2001).
- [21] B. Oksendal, *Stochastic differential equations: An Introduction with Applications*, Springer (2013).

- [22] I. Podlubny, *Fractional Differential Equations: An Introduction to Fractional Derivatives, Fractional Differential Equations, to Methods of Their Solution and Some of Their Applications*, Elsevier Science (1998).
- [23] M. Stynes, E. O’Riordan and J.L. Gracia, *Error analysis of a finite difference method on graded meshes for a time-fractional diffusion equation*, SIAM J. Numer. Anal. **55**, 1057–1079 (2017).
- [24] G. Wu, Z. Deng, D. Baleanu and D. Zeng, *New variable-order fractional chaotic systems for fast image encryption*, Chaos **29**, Paper No. 083103 (2019).
- [25] X. Wu and Y. Yan, *Milstein scheme for a stochastic semilinear subdiffusion equation driven by fractionally integrated multiplicative noise*, Fractal Fract. **9**, Paper No. 314 (2025).
- [26] Z. Yang, X. Zheng and H. Wang, *A variably distributed-order time-fractional diffusion equation: Analysis and approximation*, Comput. Methods Appl. Mech. Eng. **367**, Paper No. 113118 (2020).
- [27] F. Zeng, Z. Zhang and G.E. Karniadakis, *A generalized spectral collocation method with tunable accuracy for variable-order fractional differential equations*, SIAM J. Sci. Comput. **37**, A2710–A2732 (2015).
- [28] X. Zheng, *Two methods addressing variable-exponent fractional initial and boundary value problems and Abel integral equation*, CSIAM Trans. Appl. Math **6**, 666–710 (2025).
- [29] X. Zheng, Y. Li and W. Qiu, *Local modification of subdiffusion by initial Fickian diffusion: Multiscale modeling, analysis, and computation*, Multiscale Model. Simul. **22**, 1534–1557 (2024).
- [30] X. Zheng and H. Wang, *Optimal-order error estimates of finite element approximations to variable-order time-fractional diffusion equations without regularity assumptions of the true solutions*, IMA J. Numer. Anal. **41**, 1522–1545 (2021).
- [31] P. Zhuang, F. Liu, V. Anh and I. Turner, *Numerical methods for the variable-order fractional advection-diffusion equation with a nonlinear source term*, SIAM J. Numer. Anal. **47**, 1760–1781 (2009).